Optical Clock Sources based on Two-Section Distributed Feedback Laser with Shift-Layer

Jer-Shien Chen[1] and Hong-Chang Kung[2]
[1]Graduate Institute of Communication Engineering, National Taiwan University, Taipei, R.O.C. e-mail: d91942012@ntu.edu.tw
[2]*Electrical Engineering Department of Tung Nan Institute of Technology, Taipei, Taiwan, R.O.C.*

Abstract— **We propose a numerical model to estimate the self-sustained pulsation frequency, matched to the measured pulsation frequency, which considers the structure factors in a two-section distributed feedback laser with a thin shift-layer.**

I. Introduction

Optical re-timing is one of the key factors in all-optical networks. Optical clock recovery (OCR), which is usually based on an optical clock source, is essential for optical re-timing. Among the existing solutions for OCR, an optical clock source based on the self-sustained pulsation (SSP) mechanisms in laser diodes is very attractive due to its compact size and potentially low cost [1]. Two main mechanisms, dispersive-Q-switching (DQS) and Mode Competition [2], have been studied extensively. However, research on SSP often fails to develop a simple model for estimating the SSP frequency (s.p.f). So, the optical clock source design still faces one difficulty of try-and-error and the importance of structure parameters has not been compared. This is mainly due to the lack of a suitable modulation transfer function (MTF) for the mechanism to estimate the s.p.f. Fewer reports focus on pulsation frequency prediction [3].

In order to solve these problems, in this paper, we propose a simple model for estimating the s.p.f. of a two-section DFB (TS-DFB) laser with a built-in Bragg-wavelength-detuned (BWD) laser, i.e. shift-layer, so that try-and-error development can be avoided. The model includes two main parts: Modulation Transform Function as the first part, and SSP Condition as the second part.

II. Modulation Transform Function (MTF, First Part)

The TS-DFB laser has a structure similar to that of a conventional DFB laser, except that a thin shift-layer is grown atop the grating layer and removed for one section [4]. The TS-DFB laser is biased to have a laser section and a reflector section. The reflector section is biased below the threshold current, while the laser section is biased well above the threshold current. The section with a shift-layer has a larger effective index and thus a longer Bragg wavelength. The Bragg wavelength detuning gives rise to the offset of the lasing modes. Such a design breaks the mode degeneracy of DFB lasers and provides stable single mode output. For the TS-DFB with a shift-layer, we define the section length ratio, s.l.r., as the ratio of the section length with the shift-layer to the section length without the shift-layer.

When we want to observe how lasers behave dynamically such as a modulation of some parameter, small signal responses of one variable in term of a perturbation can be accommodated by taking differential of rate equations. Under Langevin noise approach, we could make use of the differential rate equation (1), an it is like a second order differential equation; where where N_i is the electron density in the section i, with i=1,2; N_p is the photo density, v_{gi} the group velocity, τ the carrier lifetime, F_N the Langevin noise. The gain variation can be future expanded by assuming that it is affected by the both carrier and photon density variation [5]. Several coefficients could be introduced to allow us to conveniently describe the differential rate equations and to transfer these equations into frequency domain in a compact 3x3 matrix form, as shown in equation (2). By using the Crammer's Rule, we can get the MTF as a third-order characteristic function, shown in equation (3). A_i, B_i, and c_{ij}, are coefficients.

$$\frac{d}{dt}(dN_i(t)) = -d\left(\frac{N_i(t)}{\tau} + v_g g(t) N_p(t)\right) + F_N(t) \tag{1}$$

$$\begin{pmatrix} c_{11}+j\omega & 0 & c_{13} \\ 0 & c_{22}+j\omega & c_{23} \\ -c_{31} & -c_{32} & c_{33}+j\omega \end{pmatrix} \begin{pmatrix} N_1(\omega) \\ N_2(\omega) \\ N_p(\omega) \end{pmatrix} = \begin{pmatrix} F_{N_1}(\omega) \\ F_{N_2}(\omega) \\ F_{N_p}(\omega) \end{pmatrix} \tag{2}$$

$$H(s) = \frac{B_1 + B_2 s + B_3 s^2}{A_1 + A_2 s + A_3 s^2 + s^3} \tag{3}$$

While the carrier density changes quickly, it is reasonable to conclude that the MTF will have a peak on the s.p.f. if the pulsation stability condition is satisfied. The pulsation stability condition will be studied in the second part of the proposed model. A higher carrier density change slope may lead to a higher s.p.f. We can plot the three-pole function after replacing the parameters with the practical value. Therefore, the first part of the proposed model has been established.

III. SSP Condition for TS-DFB (Second Part of the Model)

To obtain the oscillation condition, we assume small perturbations of the equilibrium photon and carrier densities. These variables can then be written as the sum of the steady-state quantities, with a small deviation shown as equations (4a)~(4b), where N_i is the electron density in the section i, with i=1,2; N_p is the photo density, N_{si} , N_{op} are the static values, and ΔN_i, ΔN_p are their corresponding deviations. By inserting equations (4a)~(4b) into rate equations, neglecting second and higher-order terms, we obtain the equations for the signal perturbation. Then, we rearrange equations into a 3x3 matrix, shown as equation (5); and it is like three first-order differential equations. Then, using multi-variables as replacements is a good approach. All three equations can be merged into a third-order differential equation in a single variable. The third-order equation can be

transferred into Laplace domain (S-domain), i.e., $s^3 + C_2 s^2 + C_1 s^1 + C_0 = 0$.

$$N_i(t) = N_{si}(t) + \Delta N_i(t) \quad (4a) \qquad N_p(t) = N_{op}(t) + \Delta N_p(t) \quad (4b)$$

$$\begin{pmatrix} \frac{d[N_1(t)]}{dt} \\ \frac{d[N_2(t)]}{dt} \\ \frac{d[N_p(t)]}{dt} \end{pmatrix} = \begin{pmatrix} e_{11} & 0 & e_{13} \\ 0 & e_{22} & e_{23} \\ e_{31} & e_{32} & e_{33} \end{pmatrix} \begin{pmatrix} N_1(t) \\ N_2(t) \\ N_p(t) \end{pmatrix} \quad (5)$$

Figure 2 is the equivalent chart in the S-domain. It is matched to the property of TS-DFB SSP that is the periodic output is generated by the laser itself when the coefficients C_2, C_1, and C_0 are appropriate. From Routh-Hurwitz criterion in automatic control theory, we can observe that the SSP criterion should be shown as $C_2C_1 \fallingdotseq C_0$ [2].

Figure 3 and figure 4 show how the MTF and the SSP condition co-work. Figure 3 shows the radio frequency from the MTF; carrier density sweeps and the other parameters are fixed. The MTF shows a frequency range that may comprise SSP. However, this is not all; the higher range of the frequency still should satisfy the Routh-Hurwitz criterion. Figure 4 shows the calculated s.p.f. from the MTF while the Routh-Hurwitz criterion is met. The frequency position for quick photon density change is about equal to the s.p.f. The s.p.f. is about 5.8GHz. Figure 5 and figure 6 show the simulated SSP region under a carrier density 2D plane, i.e. the vertical axis is N_1 and the horizontal axis is N_2. The total length is 400um, and the s.l.r. is 2; that is, L_1 is the long section, i.e. 800/3um, corresponding to N_1, and L_2 is the short section, i.e. 400/3um, corresponding to N_2. Colored areas, including triangle tags on the boundary, in the both figures, are the SSP regions. In Fig. 5, it is the case, $N_2 >> N_1$; in Fig. 6, it is the case, $N_1 >> N_2$. In addition, if we let the two SSP regions in a 2D plane figure, the SSP regions are very small which is also matched to the well known results that it is difficult to tune injection current for SSP. The carrier densities are similar to the case of asymmetric injected currents; i.e. the carrier densities plane also shows a strong asymmetric property.

IV. Importance Evaluation of Structural Parameters

Several parameters, i.e. grating coupling coefficient, s.l.r, carrier density, and effective group refractive index, usually appear in SSP condition and the MTF. If one parameter changes and creates a larger possible s.p.f range, then the parameter is a more important role in the SSP architecture. Moreover, density and cavity length exhibit an interaction effect; hence, it is difficult to separate their real effects. The better solution is to use s.l.r. as the sweep parameter, instead of the individual length. For save space, in this paper, only the corresponding relationship between the change percentage of the refractive index caused by adding purely the shift-layer and the s.l.r, as shown in fig. 7. For example, it is reasonable to consider that the refractive index difference could be changed from 3.277 to 3.2775. All other parameters are fixed. It shows one trend, that the change percentage of refractive index is not greatly affected. This figure shows a very small SSP frequency tuning range, i.e. less than 1GHz. Hence, it is clear that the s.l.r. is more important than the change percentage of the refractive index.

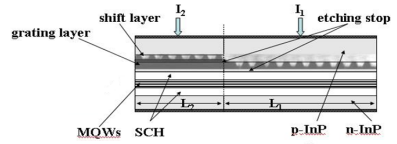

Fig. 1. TS-DFB architecture with a thin shift-layer grown atop the grating layer and removed for one section.

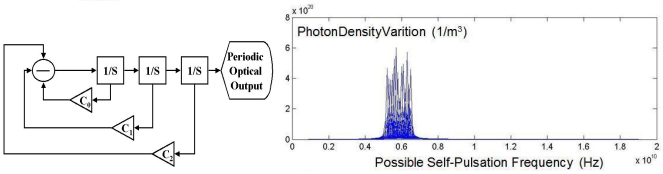

Fig. 2(left). The equivalent signal model in the S-domain. It is matched to the property of TS-DFB SSP that the periodic optical output waveform is generated by the laser itself if $C_2C_1 \fallingdotseq C_0$. Fig .3(right). The possible SSP range from the MTF; the range is from 4GHz to 8GHz (the unit of horizontal axis is 10^{10} Hz). The vertical axis is the photo density variation (its unit is $10^{20}/m^3$).

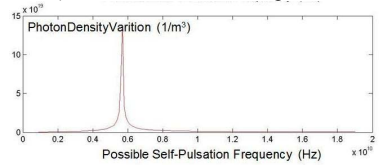

Fig .4. The calculated SSP frequency suitable to pulsation condition; its value is about 5.8GHz (the unit of horizontal axis is 10^{10} Hz). The vertical axis is the photo density variation (its unit is $10^{19}/m^3$).

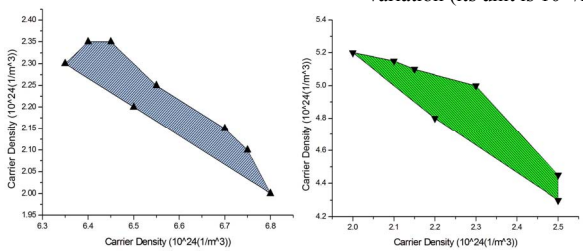

Fig. 5(left). Simulated SSP region under a carrier density 2D plane, i.e., the vertical axis is N_1 and the horizontal axis is N_2. It is the case of $N_2 >> N_1$; i.e., the carrier density in the short section, L_2, is much higher than that in the long section, L_1. Colored areas, including triangle tags on the boundary, in the both figures are the SSP region. Unit of both axes is $10^{24}/m^3$.

Fig. 6(right). Simulated SSP region under a carrier density 2D plane, i.e., the vertical axis is N_1 and the horizontal axis is N_2. It is the case of $N_1 >> N_2$; i.e., the carrier density in the long section, L_1, is much higher than that in the short section, L_2. Colored areas, including triangle tags on the boundary, in the both figures, are the SSP regions. Unit of both axes is $10^{24}/m^3$.

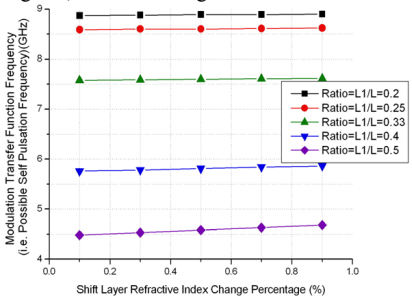

Fig. 7. Importance comparison between refractive index change percentage and the length ratio. The change percentage of refractive index is not greatly affected. This figure shows a very small SSP frequency tuning range, i.e. less than 1GHz. In addition, L equals to L1+L2.

V. Conclusion: In this paper, we derive a numerical model, including MTF of 3x3 matrix and SSP condition, so that we can estimate the possible s.p.f. Moreover, we perform importance analysis of different structure parameters.

References

[1] P.E. Barnsley, H.J. Wickes, G.E. Wickens, and D.M. Spirit, "All-optical clock recovery from 5 Gb/s RZ data using a self-pulsating 1.56 μm laser diode," IEEE Photonics Technology Letters, *Vol. 3, pp. 942-945, Oct. 1991.*

[2] Guillaume Pham and Guang-Hua Duan, "Self-pulsation in two-section DFB semiconductor lasers and its synchronization to an external signal," IEEE Journal of Quantum Electronics, *Vol.34, No.6 , pp.1000-1008, June 1998.*

[3] M. Al-Mumin, "The Effect of Gain-Coupling on Mode Beatings in Weakly Coupled Two-Section DFB Lasers," *in Tech. Digest of 7th International Conference on Numerical Simulation of Optoelectronic Devices, pp.71-72, 24-27 Sept. 2007.*

[4] San-Liang Lee, Chih-Jen Wang, Pei-Ling Jiang, Ing-Fa Jang, Hong-Wei Chang, Chiu-Lin Yao, Chia-Chien Lin, Wen-Jeng Ho, Xingang Zhang, and Yu-Heng Jan, "Two-Section Bragg-Wavelength-Detuned DFB Lasers and Their Applications for Wavelength Conversion," IEEE Journal of Selected Topics in Quantum Electronics, *Vol.11, No.5, pp.1153-1161, Sep. 2005.*

[5] Larry A. Coldren and Scott W. Corzine, *Diode Lasers and Photonic Integrated Circuits*. New York: John Wiley & Sons Inc, 1995, ch. 5 and appendix 13.